Shear-Induced Interfacial Structure of Isotactic Polypropylene (iPP) in iPP/Fiber Composites

X. Sun,† H. Li,* J. Wang, and S. Yan*

Beijing National Laboratory for Molecular Sciences, State Key Laboratory of Polymer Physics and Chemistry, Institute of Chemistry, The Chinese Academy of Sciences, Beijing 100080, People's Republic of China

Received September 10, 2006; Revised Manuscript Received October 8, 2006

ABSTRACT: The shear-induced interfacial structure of iPP in pulled iPP/fiber composites was studied by optical microscopy. Although the Kevlar fiber shows basically no nucleation ability for the iPP in quiescent melt under chosen conditions, different interfacial morphologies have been observed by pulling the fiber embedded in the matrix. It was found that the polymorphic nature of cylindrites developed on the sheared layer along the fiber strongly depended on the fiber-pulling rate, the duration of pulling, and the temperatures used for fiber pulling and subsequent crystallization. At lower fiber-pulling rates, α-iPP cylindrites were always the observed morphologies no matter how long the fiber was pulled. At moderate pulling rates, the interfacial morphologies varied from pure α-iPP cylindrites, to mixed α- and *β*-iPP cylindrites, and finally to the *β*-iPP cylindrites, depending on the pulling time. At higher fiber-pulling rates, *β*-cylindrite structures of iPP were the observed morphologies. According to the observed morphological features, it is suggested that there exists an orientation window of the iPP molecules in the molten state, which enables the formation of *β*-iPP crystals.

Introduction

Isotactic polypropylene (iPP), one of the most widely studied polyolefins, exhibits pronounced polymorphisms and morphologies depending on its tacticity, thermal treatment, and mechanical handling. Among the known crystalline forms of iPP, the *β*-iPP crystal demonstrates different characteristics from its other counterparts, e.g. low crystal density, low melting temperature, and low fusion enthalpy, but has remarkably improved impact strength and toughness.[1−3] Unfortunately, the *β*-iPP is difficult to obtain under normal processing conditions since its nucleation occurs much more rarely in bulk crystallization than that of α-modification. Therefore, special crystallization procedures, such as crystallization with specific nucleation agents or under temperature gradient, were usually used for obtaining *β*-iPP. Moreover, it was found that a sheared or strained melt encouraged the formation of *β*-iPP.[1−2,4−10] Therefore, the crystallization of iPP under a shear field has been the object of intense interest since a shear field on the polymer melts can be developed in most of the polymer processing operations. Through systematic studies,[11−15] great effort and progress have been made on shear-induced crystallization of iPP concerning the crystallization kinetics and structure development. The formation mechanism of the *β*-iPP crystals is, however, not clear. To elucidate the origin of *β*-iPP crystallization, a fiber-pulling technique was developed, in which the shear-induced crystallization of iPP was performed by pulling the fiber embedded in iPP melts along the fiber axis.[16−18] It was attested that the fiber-pulling process was efficient in producing samples rich in *β*-modification. Through selective melting of the *β*-iPP crystals at temperatures above the melting point of *β*-iPP but below that of α-iPP (e.g. 160 °C), a thin α-iPP layer directly connected to the pulled fiber with a zigzag outline was observed. On the basis of this fact, it was concluded that shearing the iPP melt by fiber pulling yielded primary α-row nuclei along the fiber.[6] As shown in Figure 1, on the surface of these α-row nuclei, an α-to-*β* growth transition or α*β*-bifurcation took place during crystal growth, which led to the formation of randomly dispersed *β*-nuclei. These *β*-nuclei could induce a layer enriched in the *β*-phase along the pulled fiber as long as the kinetic requirement for a higher growth rate of the *β*-phase (G_β) than α-phase (G_α) was achieved.[6,8,19−21] Otherwise, the quickly growing α-iPP crystals would have embedded the generated *β*-nuclei. The questions which remain difficult to be understood are (i) that the occurrence of α*β*-bifurcation on the surface of the in situ formed α-row nuclei rather than a growth of α-iPP crystals and (ii) the original morphological difference on the α-row nuclei surface between the places where α*β*-bifurcation was taking place and the growth of α-iPP crystals, i.e., the bottom edges of the α-iPP triangles. In other words, the origin behind the α*β*-bifurcation is still not quite clear. Li et al.[15] claimed that shear could induce ordered smectic domains and argued that growth of *β*-iPP crystals from smectic bundles induced by shear should be easier than from α-iPP row nuclei having regular right- and left-handed helical packing. On the basis of this consideration, they concluded that ordered smectic

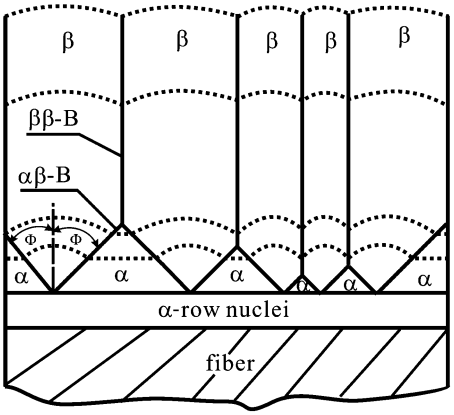

Figure 1. Schematic diagram of a cylindrite structure with α*β* bifurcation.

* To whom all correspondence should be addressed. E-mail: skyan@iccas.ac.cn. Tel 0086-10-82618476. Fax 0086-10-82618476.

† Ph. D. candidates of the Chinese Academy of Sciences.

10.1021/ma062105d CCC: $33.50
Published on Web 11/17/2006

bundles rather than α-iPP row nuclei initiated the growth of β-iPP crystals. Somani et al.,[22] however, did not find any traces of the smectic phase during the study on the shear-induced crystallization by in situ synchrotron wide-angle X-ray diffraction. They found instead that the β-crystals grew only after the formation of oriented α-crystals. Therefore, further study on the origin of β-iPP crystallization is clearly warranted.

Our previous work on self-induced crystallization of iPP indicates that partial melting of the iPP fiber favors the formation of β-iPP crystals. This may imply that the formation of β-iPP is related to the chain orientation of the iPP in its molten state.[23−27] To get further insight into the formation of β-nuclei in a sheared iPP melt, the dependence of interfacial supramolecular structure in the pulled fiber/iPP systems on the fiber-pulling rate, which was uncovered by the written sources consulted, was studied in the present work. The purpose of this paper is to present some detailed experimental results concerning the shear-induced interfacial structure of iPP in the iPP/fiber composites.

Experimental Section

The matrix material used in this work was commercial grade isotactic polypropylene (iPP), GB-2401, with a melt flow index of 2.5 g/10 min, an M_w of 4.4×10^5 g/mol, and a melting temperature of 170 °C, produced by Yanshan Petroleum and Chemical Corp., China. The granular iPP materials were used without any further treatment. Thin iPP films, 30−40 μm in thickness, were prepared by compression-molding the iPP granules at 200 °C.

To study the shear-induced crystallization of iPP in the fiber-pulling system, a single Kevlar fiber (Kevlar 49, Dupont, Wilmington, DE) with a radius of ca. 5 μm was sandwiched between two pieces of the compression-mold iPP thin films and pressed again by a homemade small hot stage at 210 °C for 5 min to erase the possible effects of thermal history on the subsequent crystallization. The sample was then cooled quickly to 137 °C, at which the fiber was pulled along the fiber axis. After the fiber was pulled at a different rate for certain duration, the iPP was then crystallized isothermally at 137 °C for various periods of time, and finally cooled in air to room temperature. The pulling process was conducted at a homemade fiber-pulling system with controlled pulling rates ranging from 0 to 700 μm/s.

For morphological observation, an Olympus BH-2 optical microscope equipped with a Linkam LTS 350 hot stage was used in this study. The optical micrographs shown in this paper were all taken under crossed polarizers.

Results

First reported here is the nucleation ability of Kevlar 49 fiber toward quiescent iPP melts. For a direct comparison, the exact same thermal treatment used for fiber-pulling experiments was used for the sample preparation: namely, the iPP sample containing a single Kevlar 49 fiber was first heat-treated at 210 °C for 5 min to remove its thermal history and then cooled to 137 °C for isothermal crystallization. Figure 2 shows the optical micrograph of the resultant morphology. One can easily recognize that the nucleation density of iPP on the Kevlar 49 fiber surface is similar to that in the matrix. This indicates that the Kevlar 49 fiber exhibits no nucleation ability toward the quiescent iPP melts. The result seems different from the those reported in the literatures,[6,16,28−31] where the effect of Kevlar fiber on the nucleation of iPP is clearly identified. This is actually caused by different crystallization temperatures used in the experiments.

Figure 3a shows an optical micrograph of the iPP/Kevlar samples with the Kevlar 49 fiber being continuously pulled at 137 °C for 20 s with a pulling rate of 30 μm/s and then crystallized isothermally at the same temperature for 2 h. Compared to Figure 2, it is obvious that there is a remarkable increment in the nucleation density of iPP on the Kevlar fiber surface. The enhanced nucleation ability of Kevlar 49 fiber toward iPP caused by fiber pulling leads to the formation of a cylindrite interfacial structure around the Kevlar fiber as reported by Thomason et al.[16] The selective melting test indicates that

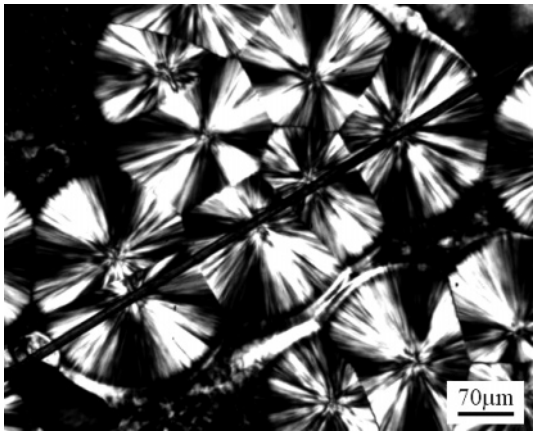

Figure 2. An optical micrograph shows the interfacial morphology of an iPP and Kevlar fiber composite sample, which was heat-treated at 210 °C for 5 min to remove its thermal history and then cooled to 137 °C for isothermal crystallization in a quiescent environment.

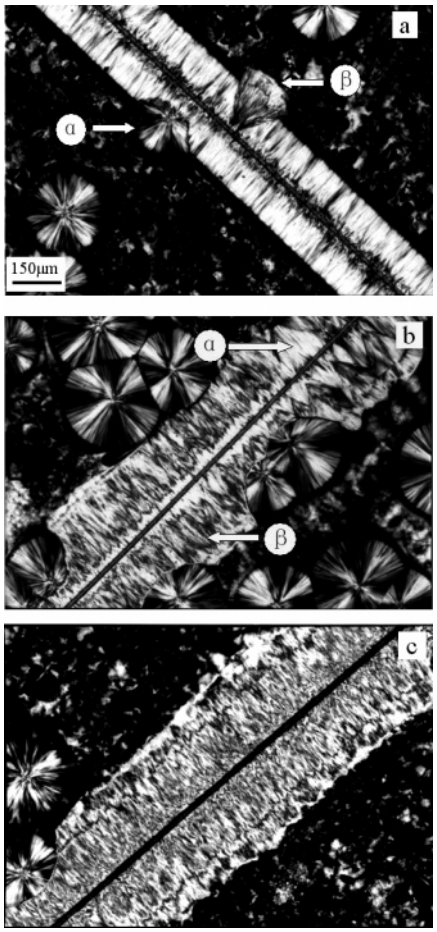

Figure 3. Optical micrographs illustrate the interface morphologies of the iPP and Kevlar fiber systems. The samples were heat-treated at 210 °C for 5 min and then quickly cooled to and kept at 137 °C for fiber pulling at a rate of 30 μm/s. The fiber-pulling times were: (a) 20 s, (b) 35 s, and (c) 60 s. After fiber pulling, the samples were isothermally crystallized for 2 h.

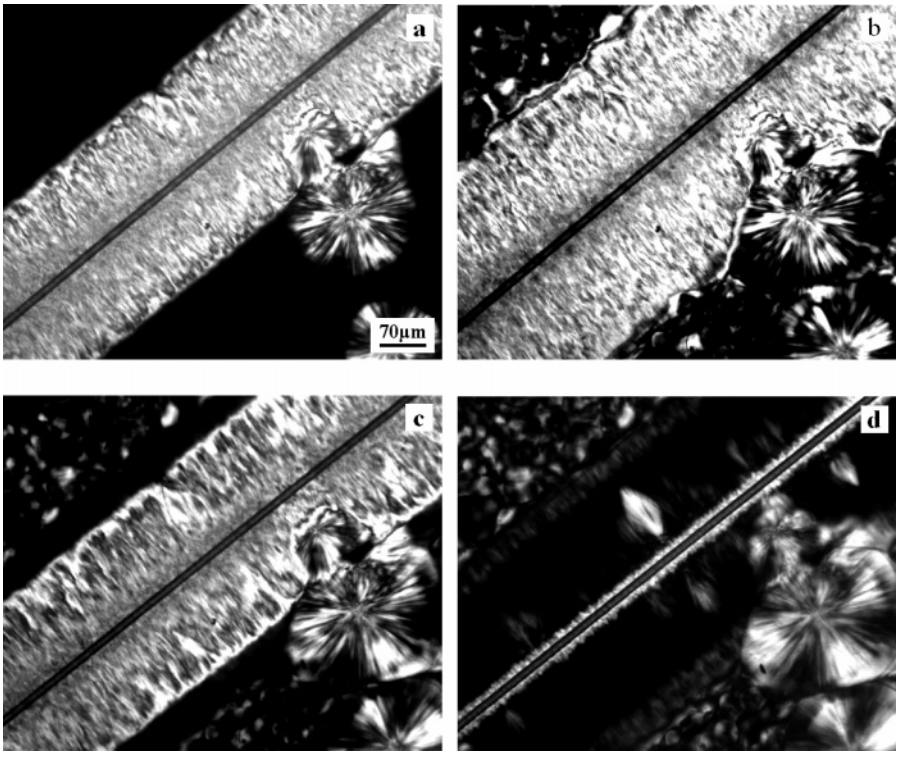

Figure 4. Optical micrographs taken during the crystallization and subsequent melting processes of an iPP/fiber system similar to that used in Figure 3d. The isothermal crystallization time is 1 h. After that the sample was first cooled to room temperature in air and then reheated at a rate of 10 °C/min to 158 °C. (a) Isothermally crystallized at 137 °C 1 h, (b) cooled to room temperature, (c) reheated to 153 °C, and (d) reheated to 158 °C.

the resultant cylindrite structure around the fiber is composed basically of α-iPP crystals. Some fan-shaped β-iPP microdomains sporadically dispersed in the α-iPP column layers can be occasionally observed, such as the one existing in Figure 3a indicated by a white arrow labeled "β". Comparing with the growth front of the cylindrite composed of α- and β-crystals, one can recognize that the β-iPP crystal clearly grows more quickly than its α counterpart. The observed morphological feature is different from that observed by Varga et al.[6] They reported that the existence of shear stress produced by fiber pulling promoted the formation of cylindritic structures of β-iPP. The formation of β-cylindrites is limited in a temperature interval with a lower ($T_{\alpha\beta} \approx 100$ °C) and an upper ($T_{\beta\alpha} \approx 140$ °C) threshold to meet the kinetic requirement of $G_\beta > G_\alpha$, where G_β and G_α represent the crystal growth rate of β- and α-iPP, respectively. The content of the iPP β-modification is highest when crystallization temperature (T_c) and fiber-pulling temperature (T_{pull}) are closely matched within this temperature range, i.e., $T_{\alpha\beta} < T \approx T_{pull} < T_{\beta\alpha}$. This is not affected by the nucleation ability and the nature of the fibers used. In the present case, even though the fiber-pulling temperature is exactly the same as the crystallization temperature and well within the aforementioned temperature range, a cylindrite interfacial structure composed basically of α-iPP crystals is observed.

The interfacial structure of iPP around Kevlar fiber was found to vary with the fiber-pulling time. With an increase in fiber-pulling time, as shown in parts b and c of Figure 3, the interfacial morphology changes a lot. When pulling the fiber at the same rate for 35 s, a cylindrite structure rich in β-iPP crystals is observed (see Figure 3b). Nevertheless, some triangular α-iPP domains can be seen, as indicated with an arrow labeled "α". Also, narrow α-iPP layers of several microns inserted between the Kevlar fiber and the resultant β-iPP crystals can be identified. When pulling the fiber at a rate of 30 μm/s for 60 s, cylindrite interfacial structure with strong birefringence is observed, as shown in Figure 3c. The selective melting test demonstrates that the cylindrite structure is composed predominately of β-iPP crystals. Moreover, in Figure 3c, the β-cylindrite can be divided into two layers with different birefringence, i.e., the inner and outer layers. This can also be identified in the α-cylindrite shown in Figure 3a with careful inspection. These outer surrounding layers are formed during the cooling process of the sample after isothermal crystallization, as verified by in situ observation of the crystallization and melting processes of the sample. Figure 4 presents some of the optical micrographs taken during the crystallization and melting processes. The sample was prepared by pulling the Kevlar 49 fiber at 137 °C for 60 s with a pulling rate of 30 μm/s, then allowing it to crystallize isothermally for 1 h, and finally cooling it to room temperature. From Figure 4a, it is found that β-iPP cylindrite of approximately 150 μm can be formed after 1 h of isothermal crystallization. During the cooling process, a ca. 40 μm extension of the preformed β-iPP cylindrite has been developed, as shown in Figure 4b. Meanwhile, some microcrystallites in the matrix far away from the fiber have also been developed. When the sample was heated again, the latter-formed β-iPP cylindrite layer melted at 153 °C, as in Figure 4c, indicating that this layer is indeed composed of β-iPP crystals. This part of the crystals grows at a relatively lower temperature and therefore has a lower melting temperature. The inner part of the β-cylindrite melts at 158 °C, and the early molten outer part recrystallizes in its α-form, as shown in a comparison of Figure 4d with 4c. The melting of the β-iPP results in a clear display of the α-iPP crystals previously inlaid in the β-cylindrite and the "saw-tooth" shaped α-iPP crystals around the fiber, as shown in Figure 4d. This observation is consistent with the findings of Varga et al.[6]

The above results indicate that the aforementioned deviation between our and Varga's observation may be caused by a different fiber-pulling rate. The pulling rate used here should be smaller than that used in the cited work,[6] where the fiber

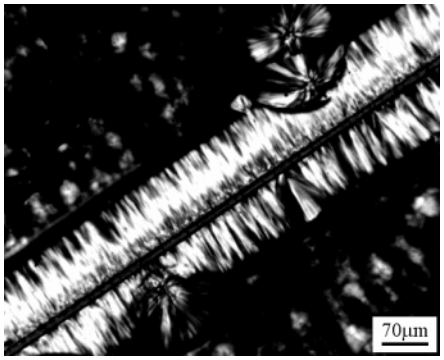

Figure 5. An optical micrograph illustrates the interface morphology of an iPP/fiber composite, which was heat-treated at 210 °C for 5 min and then quickly cooled to and kept at 137 °C for fiber pulling at a rate of 17 μm/s for 10 min and subsequent isothermal crystallization for 2 h.

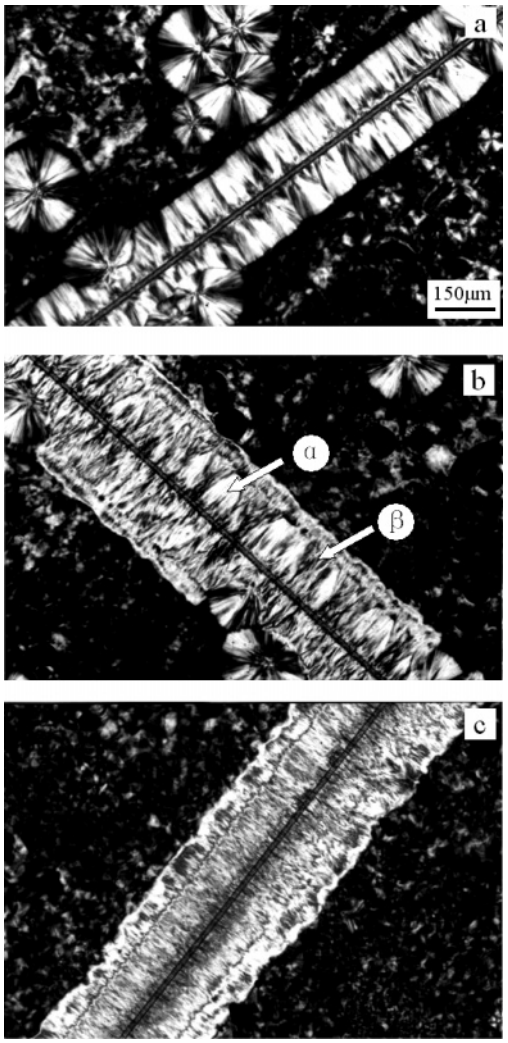

Figure 6. Optical micrographs illustrate the interface morphologies of the iPP and Kevlar fiber systems. The fibers were also pulled at 137 °C with a rate of 93 μm/s for (a) 3, (b) 10, and (c) 15 s. After the fiber pulling, the samples were isothermally crystallized for 2 h at 137 °C.

was pulled manually. To confirm this, an even lower fiber-pulling rate, i.e., 17 μm/s, was selected, with the temperature of fiber pulling and subsequent crystallization remaining unchanged. In this case, as shown in Figure 5, interfacial cylindrites of α-iPP were always the observed morphologies, regardless of the fiber-pulling time. The maximum fiber-pulling time used was 10 min. This clearly indicates that the shear-induced final interfacial morphology of iPP depends strongly on the fiber-pulling rate. Therefore, the influence of the fiber-pulling rate on the resultant interfacial structure was studied. Figure 6 presents the optical micrographs showing the interfacial morphologies of samples with the fiber pulled at a rate of 93 μm/s for 3, 10, and 15 s, then isothermally crystallized at 137 °C for 2 h, and finally cooled to room temperature. The produced interfacial structures that these three pictures show are quite different. With a short fiber-pulling time, i.e., 3 s, the interfacial cylindrite structure was composed only of α-iPP crystals (see Figure 6a). When the pulling time was increased to 10 s, a mixed morphology of α- and β-crystals with the fan-shaped β-crystals inlaid in the α-cylindrite appeared along the fiber, as shown in Figure 6b. With further increase in the fiber-pulling time, i.e., to 15 s, β-cylindrite is generated (see Figure 6c). Combining Figure 6 with Figure 3, one can note that with higher fiber-pulling rate, a shorter fiber-pulling time is required for generating β-iPP cylindrites. This is reasonable since a high degree of chain orientation can be achieved in short time with a high shear rate.

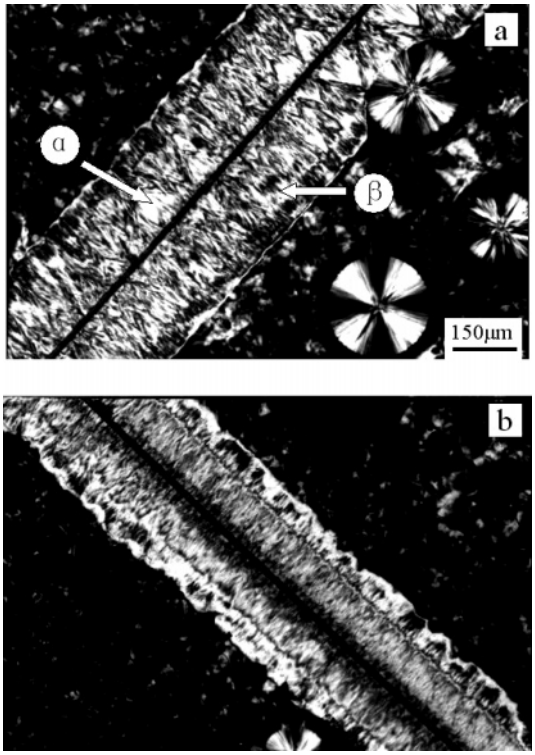

Figure 7. Optical micrographs illustrate the interface morphologies of the iPP and Kevlar fiber systems. The samples were heat-treated at 210 °C for 5 min and then quickly cooled to and kept at 137 °C for fiber pulling at a rate of 200 μm/s. The fiber-pulling times were: (a) 5 s, and (b) 10 s. After fiber pulling, the samples were isothermally crystallized at 137 °C for 2 h.

When the fiber-pulling rate was increased to 168 μm/s, similar results to the case of 93 μm/s were obtained. The interfacial structure also experiences the transition from pure α-cylindrite through an $\alpha\beta$ coexisting state to the β-cylindrite with the increase of fiber-pulling time. The time window for producing pure α-cylindrite is, however, much narrower compared with the case of 93 μm/s. In other words, β-iPP crystals are produced at an even shorter fiber-pulling time. When the pulling rate was set at 200 μm/s, no pure α-cylindrite structure was observed in our experimental procedure at all. As shown in Figure 7, only 5 s pulling of the fiber produces an interfacial structure rich in β-modification of iPP (see Figure 7a). For 10 s pulling of the fiber, Figure 7b, no α-iPP crystal can be identified under optical

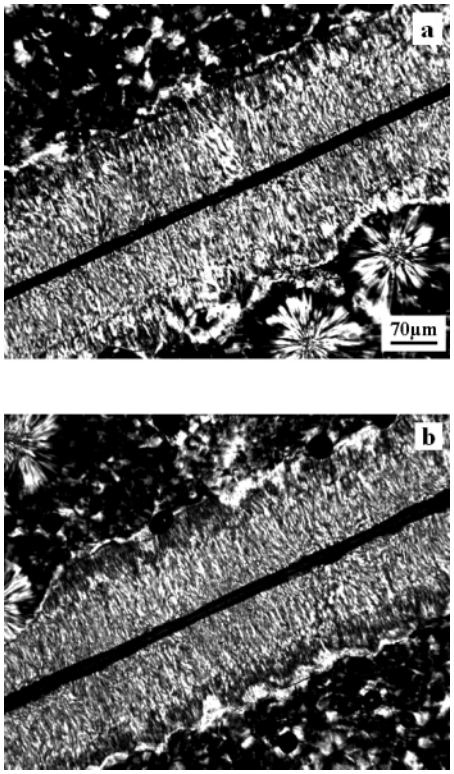

Figure 8. Optical micrographs illustrate the interface morphologies of the iPP and Kevlar fiber systems with the fibers pulled at 137 °C for only 1 s. The fiber-pulling rates were (a) 233 μm/s and (b) 515 μm/s. After the fiber pulling, the samples were isothermally crystallized at 137 °C for 1 h.

microscope resolution. If a fiber-pulling rate higher than 233 μm/s is used, even shorter fiber-pulling time (e.g. 1 s) can already initiate the formation of highly ordered β-cylindrites, and no noticeable difference between the induced interface morphology can be distinguished under optical microscope, as shown in Figure 8.

On the basis of the above observation, it is clear that interfacial β-cylindrites can be produced by either a long fiber-pulling time with relatively lower pulling rates or a short fiber-pulling time with higher pulling rates. Under an optical microscope based on birefringence, the appearances of these interfacial β-cylindrites are so similar that no difference can be identified through morphological observation. This is somewhat different from the earlier studies performed by Thomason et al.,[16] where only α-cylindrites were observed at all of the used experimental conditions. The reason is that the chosen isothermal crystallization temperatures in most cases are higher than 140 °C, which is beyond the kinetic requirement for inducing β-crystallization of iPP. Only in one case the isothermal crystallization temperature was set at 134 °C, well within the temperature window for producing β-crystals; the chosen pulling rate was, however, only 0.025 mm/min (about 0.4 μm/s), which is too slow to induce β-crystallization as attested in the present work.

Discussion

From above experimental results, it is concluded that the shear imposed on the melt by fiber pulling has remarkable influence on the final interfacial morphology. The Kevlar fiber has no nucleation ability to the iPP in quiescent melt under the condition used in present study. The interfacial morphologies of iPP in the pulled systems can vary, however, from pure α-cylindrites to mixed α- and β-cylindrite structure and then β-cylindrites. The polymorphic nature of cylindrites developed on the sheared layer along the fiber strongly depends on the fiber-pulling rate, the duration of pulling, as well as the temperatures used for fiber pulling and subsequent crystallization. In the temperature window with the kinetic requirement for β-iPP crystallization fulfilled, increased pulling rate or pulling time favors the formation of β-crystals. According to these results, the formation mechanism of the β-iPP can be discussed here.

It is well-known that shear flow could obviously change the molecular orientation and affect the inter- and intramolecular interaction. These are the controlling factors for the resultant morphology.[32−37] In the case of dilute solution under different type of flow,[32] it was reported that polymer chains underwent sharp transition from random coil to a fully extended chain conformation at a critical strain rate without any intermediate stable chain conformation. Regarding the entangled polymer melt, it was argued that the coil-stretch transition should also exist since the flow-induced morphologies of a pure polymer melt were attested to be similar to those produced in dilute solutions.[33] Steady shear experiments show that the fraction of oriented crystals (X_o) and their orientation extent (Herman's orientation function) in a fully crystallized sample at room temperature increase with both shear rate and shear duration.[38] At the same time, an increase in the amount of β-iPP with the increase of the oriented crystals was also obtained.[22] This leads to the conclusion that the β-crystallization of iPP is related to its chain orientation.

In our experiment, pulling the fiber introduces shear on the polymer melt adjacent to the fiber. The shear condition depends on the shear rate and duration. At a very low fiber-pulling rate (see Figure 5), the enhanced nucleation ability of the fiber on the iPP matrix leads to the formation of cylindrite interfacial structure and indicates the existence of shear exerted on the iPP melt. However, only α-iPP cylindrite structure was observed. With increasing fiber-pulling rate, an increase of β-iPP content was seen with the increase of fiber-pulling time. This was in accordance with steady shear experiments where an increase in β-iPP was seen with the increase in shear time. These results clearly indicate that a certain extent of chain orientation is required to initiate β-crystallization of iPP. Therefore, at lower fiber-pulling rate, since orientation and relaxation of polymer chains take place simultaneously during fiber pulling, the iPP chains in the molten state can hardly be oriented well enough for triggering β-crystallization. At higher fiber-pulling rate, chain orientation is fast and high degree of chain orientation can be achieved in a short time, which is beyond the chain relaxation. As a result, the highly oriented iPP chains initiated the β-crystallization. This is consistent with Hsiao's report that the degree of crystal orientation and amount of oriented crystals are higher for a short shear time at a higher shear rate than a long shear time at a lower shear rate.[38] From the above discussion, one may expect to obtain pure β-iPP crystals at an appropriate shear rate. The experimental results are, however, to the contrary. No pure β-iPP crystals have ever been produced in the steady shear experiments. Hsiao et al.[22] found that the amount of β-phase reached a plateau value at a shear rate of 57 s^{-1}. Moreover, in studies on the effect of shear rate on the crystallization behavior of iPP, An et al.[39] found that the content of the β-iPP crystals increased first quickly in the shear rate range of 0−10 s^{-1} and then increased slowly in the range of 10∼20 s^{-1}, and a maximum β-iPP crystal content was seen at a shear rate of ca. 20 s^{-1}. With further increase of the shear rate, the β-iPP crystal content dropped down slightly (see Figure

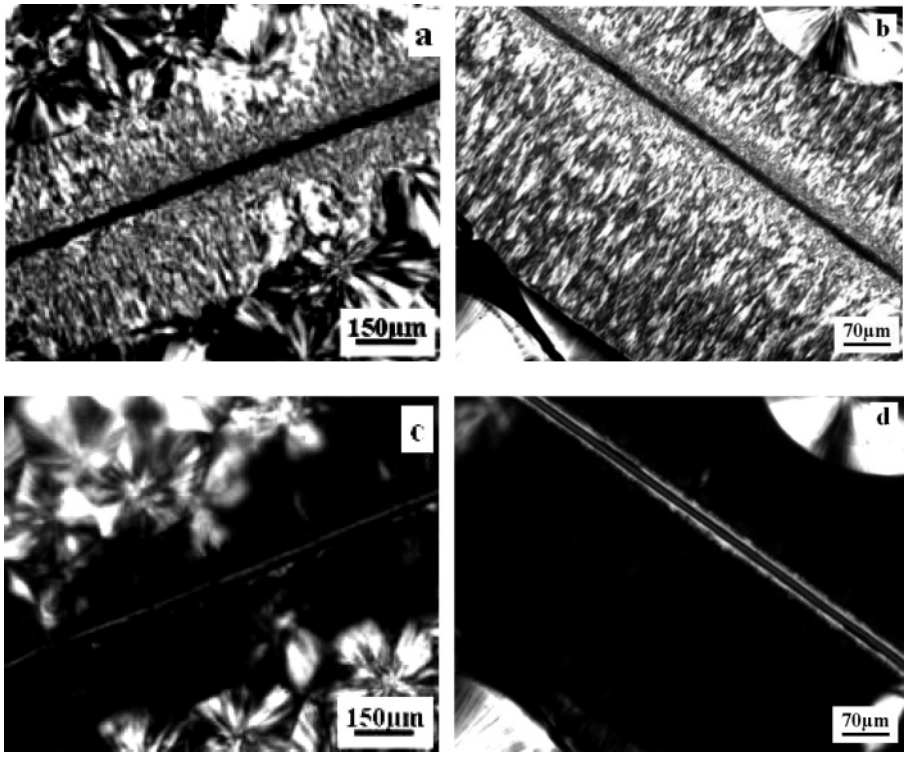

Figure 9. Optical micrographs present the interface morphologies of the iPP and Kevlar fiber systems. The samples were heat-treated at 210 °C for 5 min and then quickly cooled to and kept at 131 °C for fiber pulling and subsequent crystallization. The fibers were pulled (a) at a rate of 40 μm/s for 10 s and (b) at a rate of 515 μm/s for 1 s. The isothermal crystallization was performed at 131 °C for 2 h. Parts c and d highlight the morphologies of the residual α-crystals after selective melting at 158 °C of the samples shown in a and b, respectively.

4 of ref 39). These results may imply that only the molecules in the melt getting to a certain degree of chain orientation can promote the formation of β-modification. This is further confirmed by our selective melting experiments. Figure 9a and 9b show the optical micrographs revealing the interfacial structures of the pulled fiber systems. The samples were prepared by being heated to 210 °C for 5 min, cooled to 131 °C at which the fibers were pulled along the fiber axis, and then isothermally crystallized at 131 °C for sufficient time. The fiber-pulling rates were 40 μm/s and 515 μm/s for the samples shown in Figure 9a and 9b, respectively. From Figure 9a and 9b, it can be seen that in both cases, β-iPP cylindrite structures are produced. The dimensions of the β-iPP cylindrite layers in the direction perpendicular to the fiber axis are, however, quite different. This is related to the different chain orientation of the sheared iPP layer. At higher pulling rate, i.e., 515 μm/s, a high degree of chain orientation is achieved by fiber pulling. Consequently, an early start of nucleation and subsequent crystal growth lead to the formation of broader cylindrite structure. After selective melting of the β-iPP crystals at 158 °C, the morphologies of the remaining α-iPP crystals are very interesting. As shown in part d of Figure 9, at high fiber-pulling rate, residual saw-toothed α-crystals surrounding the fiber can be clearly observed. On the other hand, at lower fiber-pulling rate, the fiber surface in most places is quite smooth, which may indicate the absence of the saw-toothed residual α-crystals, or at least the oriented α-iPP layer is so thin that it cannot be recognized in the optical micrograph. This unambiguously indicates that the nucleation of β-iPP is governed by chain orientation in the molten state. At a higher fiber-pulling rate, a better chain orientation of the molecular chains directly in contact with the fiber is expected. This leads to the formation of the α-iPP row nuclei around the fiber. There exists an orientation gradient from the fiber surface to the unaffected matrix. In this case, the chain orientation somewhere away from the fiber may fulfill the requirement for β-nucleation and therefore leads to the $\alpha\beta$-bifurcation. From the above discussion, one may conclude that there exists a chain orientation window, in which nucleation of β-iPP crystals is preferred. Poor chain orientation is outside of this window, and α-iPP cylindrites are the produced morphology. Well oriented molecular chains beyond this window initiate primarily the oriented α-iPP row nuclei, which transform into β-nuclei through $\alpha\beta$-bifurcation. The formation of oriented α-iPP row nuclei may, however, not a prerequisite for the formation of β-iPP crystals.

Conclusion

The shear-induced interfacial structure of iPP in pulled iPP/fiber composites was studied by optical microscopy. Through varying the fiber-pulling rate and duration, a different chain orientation level of the iPP in the vicinity of the fiber can be produced, and consequently a different interfacial morphology has been observed. It has been found that the polymorphic nature of cylindrites developed on the sheared layer along the fiber strongly depends on the fiber-pulling rate, the duration of pulling, and the temperatures used for fiber pulling and subsequent crystallization. On the basis of the observed morphological features, it is suggested that there exists an orientation window of the iPP molecules in the molten state, which enables the formation of β-iPP crystals. At the very low pulling rate, e.g. 17 μm/s, the iPP chains can only be poorly oriented and outside the orientation window for β-crystallization, α-iPP cylindrites are always the observed morphology no matter how long the fiber is pulled. At a suitable pulling rate, the interfacial morphology can vary from pure α-iPP cylindrites, to mixed α- and β-iPP cylindrites, and finally to the β-iPP cylindrites, depending on pulling time. At a very high pulling rate, better chain orientation can be achieved even under slight

pulling of the fiber, and therefore β-cylindrite structures are the observed morphology.

Acknowledgment. We thank Ms. Lillian (Qiaohui) Zhou for English editing of the manuscript. Also the financial support of the Outstanding Youth Fund (No. 20425414), the National Natural Science Foundations of China (No. 50521302, 20574079, 20304018, and 20423003), and the 973 programs from MOST of China are gratefully acknowledged.

References and Notes

(1) Varga, J. *J. Macromol. Sci., Part B: Phys.* **2002**, *41*, 1121.
(2) Karger-Kocsis, J.; Moos, E.; Mudra, I.; Varga, J. *J. Macromol. Sci., Part B: Phys.* **1999**, *38*, 645.
(3) Karger-Kocsis, J. *Polym. Eng. Sci.* **1996**, *36*, 203.
(4) Leugering, H. J.; Kirsch, G. *Angew. Makromol. Chem.* **1973**, *33*, 17.
(5) Devaux, E.; Chabert, B. *Polym. Commun.* **1991**, *32*, 464.
(6) Varga, J.; Karger-Kocsis, J. *J. Polym. Sci., Part B: Polym. Phys.* **1996**, *34*, 657.
(7) Varga, J.; Ehrenstein, G. W. *Polymer* **1996**, *37*, 5959.
(8) Varga, J. Crystallization, Melting and Supermolecular Structure of Isotactic Polypropylene. In Polypropylene: *Structure, Blends and Composites*; Karger-Kocsis, J.; Ed.; Chapman & Hall: London, 1995; Vol. 1, pp 56−115.
(9) Crissman, J. M. *J. Polym. Sci.* **1969**, *7* (A2), 389.
(10) Lovinger, A. J.; Chua, J. O.; Gryte, C. C. *J. Polym. Sci., Part B: Polym. Phys.* **1977**, *15*, 641.
(11) Somani, R. H.; Hsiao, B. S.; Nogales, A.; Srinivas, S.; Tsou, A.; Sics, I.; Balta-Calleja, F. J.; Ezquerra, T. A. *Macromolecules* **2000**, *33*, 9385.
(12) Somani, R. H.; Yang, L.; Zhu, L.; Hsiao, B. S. *Polymer* **2005**, *46*, 8587.
(13) Hsiao, B. S.; Yang, L.; Somani, R. H.; Avila-Orta, C. A.; Zhu, L. *Phys. Rev. Lett.* **2005**, *94*, 117802.
(14) Li, L.; de jeu, Wim H. *Phys. Rev. Lett.* **2004**, *92*, 075506.
(15) Li, L.; de jeu, Wim H. *Faraday Discuss.* **2005**, *128*, 299.
(16) Thomason, J. L.; Rooyen, A. A. *J. Mater. Sci.* **1992**, *27*, 897.
(17) Varga, J.; Karger-Kocsis, J. *Polymer* **1995**, *36*, 4877.
(18) Varga, J.; Karger-Kocsis, J. *J. Mater. Sci. Lett.* **1994**, *13*, 1069.
(19) Varga, J.; Fujiwara, Y.; Ille, A. *Periodica Polytech. Chem. Eng.* **1990**, *34*, 255.
(20) Shi, G.; Zhang, X.; Qiu, Z. *Makromol. Chem.* **1992**, *193*, 583.
(21) Varga, J. *J. Mater. Sci.* **1992**, *27*, 2557.
(22) Somani, R. H.; Hsiao, B. S.; Nogales, A.; Srinivas, S.; Tsou, A.; Sics, I.; Fruitwala, H. *Macromolecules* **2001**, *34*, 5902.
(23) Li, H.; Liu, J.; Wang, D.; Yan, S. *Colloid Polym. Sci.* **2003**, *281*, 973.
(24) Li, H.; Jiang, S.; Wang, J.; Wang, D. J.; Yan, S. K. *Macromolecules* **2003**, *36*, 2802.
(25) Li, H.; Zhang, X.; Kuang, X.; Wang, D. J.; Li, L.; Yan, S. K. *Macromolecules* **2004**, *37*, 2847.
(26) Sun, X.; Li, H.; Zhang, X.; Wang, J.; Wang, D.; Yan, S. K. *Macromolecules* **2006**, *39*, 1087.
(27) Li, H.; Zhang, X. Q.; Duan, Y. X.; Wang, D. J.; Li, L.; Yan, S. K. *Polymer* **2004**, *45*, 8059.
(28) Wang, C.; Liu, C.-R. *Polymer* **1999**, *40*, 289.
(29) Avella, M.; Volpe, G. D.; Martuscelli, E.; Raimo, M. *Polym. Eng. Sci.* **1992**, *32*, 376.
(30) Heppenstall-Butler, M.; Bannister, D. J.; Young, R. J. *Composites, Part A:* **1996**, *27*, 833.
(31) Wu, C.-M.; Chen. M.; Karger-Kocsis, J. *Polymer* **2001**, *42*, 199.
(32) de Gennes P. G. *J. Chem. Phys.* **1974**, *60*, 5030.
(33) Keller, A.; Kolnaar, H. W. H. In Processing of polymers; VCH: New York, 1997; Meijer, H. E. H., Ed.; Vol. 18, p 189.
(34) Smith, D. E.; Babcock, H. P.; Chu, S. *Science* **1999**, *283*, 1724.
(35) Schroeder, C. M.; Babcock, H. P.; Shaqfeh, E. S. G.; Chu, S. *Science* **2003**, *301*, 1515.
(36) Schultz, J. M.; Hsiao, B. S.; Samon, J. M. *Polymer* **2000**, *41*, 8087.
(37) Samon, J. M.; Schultz, J. M.; Wu, J.; Hsiao, B.; Yeh, F.; Kolb, R. *J. Polym. Sci., Part B:* **1999**, *37*, 1277.
(38) Somani, R. H.; Yang, L.; Hsiao, B. S. *Macromolecules* **2005**, *38*, 1244.
(39) Huo, H.; Jiang, S.; An, L.; Feng, J. *Macromolecules* **2004**, *37*, 2478.

MA062105D